The EMBO Journal Vol. 21 No. 19 pp. 5302–5311, 2002

The invariant uridine of stop codons contacts the conserved NIKSR loop of human eRF1 in the ribosome

Laurent Chavatte[1,2], Alim Seit-Nebi[3], Vera Dubovaya[3] and Alain Favre[1,4]

[1]Institut Jacques Monod, UMR 7592 CNRS-Universités Paris 7–Paris 6, 2 place Jussieu, F-75251 Paris cedex 05, France and [3]Engelhardt Institute of Molecular Biology, Moscow 119991, Russia

[2]Present address: Cleveland Clinic Foundation, 9500 Euclid Avenue NC-10, Cleveland, OH 44195, USA

[4]Corresponding author
e-mail: favre@ijm.jussieu.fr

To unravel the region of human eukaryotic release factor 1 (eRF1) that is close to stop codons within the ribosome, we used mRNAs containing a single photoactivatable 4-thiouridine (s^4U) residue in the first position of stop or control sense codons. Accurate phasing of these mRNAs onto the ribosome was achieved by the addition of $tRNA^{Asp}$. Under these conditions, eRF1 was shown to crosslink exclusively to mRNAs containing a stop or s^4UGG codon. A procedure that yielded ^{32}P-labeled eRF1 deprived of the mRNA chain was developed; analysis of the labeled peptides generated after specific cleavage of both wild-type and mutant eRF1s maps the crosslink in the tripeptide KSR (positions 63–65 of human eRF1) and points to K63 located in the conserved NIKS loop as the main crosslinking site. These data directly show the interaction of the N-terminal (N) domain of eRF1 with stop codons within the 40S ribosomal subunit and provide strong support for the positioning of the eRF1 middle (M) domain on the 60S subunit. Thus, the N and M domains mimic the tRNA anticodon and acceptor arms, respectively.

Keywords: eukaryotic ribosomes/human eRF1/NIKSR region/photocrosslinking/stop codons

Introduction

Termination of translation is the last critical step of protein synthesis, as it ensures the formation of normal-sized proteins. Release of the nascent polypeptide takes place within the ribosome when the A site is occupied by the stop codon (UGA, UAA or UAG) and by class-1 polypeptide chain release factors (RF1s) (reviewed in Nakamura and Ito, 1998; Kisselev and Buckingham, 2000; Poole and Tate, 2000; Bertram *et al*., 2001). In eukaryotes, eRF1 decodes all three stop codons, whereas, in prokaryotes, RF1 and RF2 decode UAG/UAA and UGA/UAA stop codons, respectively. In response to termination codons, RF1s trigger peptidyl-tRNA hydrolysis catalyzed by the peptidyl transferase center of the ribosome. It is believed (Nakamura *et al*., 2000) that RF1s decode stop codons via direct protein–mRNA interactions, as eRF1 strongly competes with suppressor tRNAs *in vitro* and *in vivo* (Weiss *et al*., 1984; Drugeon *et al*., 1997; Le Goff *et al*., 1997) and, at least in some cases, eRF1 was shown to be in close contact with the stop codon in the ribosome (Poole and Tate, 2000; Chavatte *et al*., 2001). All known RF1s contain a ubiquitous Gly-Gly-Gln (GGQ) motif, which was found to be essential for triggering peptidyl-tRNA hydrolysis and is thought to mimic the CCA end of tRNA (Frolova *et al*., 1999; Seit-Nebi *et al*., 2001). However, the molecular basis of stop codon recognition by RF1s remains a challenging problem.

In prokaryotes, a tripeptide was inferred by mutagenesis analysis to determine RF1 stop codon recognition. Thus, Pro-Ala-Thr in RF1 and Ser-Pro-Phe in RF2 were shown to be involved in the discrimination between the second and third purine bases of the stop signal (Ito *et al*., 2000; Nakamura *et al*., 2000). Yet, the recent crystal structure of RF2 (Vestergaard *et al*., 2001) failed to support the implication of these residues in the interaction with stop codons. To study RF2–mRNA contacts occurring in *Escherichia coli* ribosomes, Tate and colleagues performed site-directed crosslinking experiments (Tate *et al*., 1990; Brown and Tate, 1994; Poole *et al*., 1997) using mini-mRNAs in which the U residue of the stop signal was replaced by its photoactivatable analog, 4-thiouridine (s^4U) (Favre *et al*., 1998). Both s^4UAA and s^4UGA (but not the non-cognate s^4UGA) 36mer mRNAs appropriately programmed on *E.coli* ribosomes by $tRNA^{Ala2}$, were shown to crosslink to RF2. Further experiments, however, demonstrated that the nature of the phasing tRNA strongly influences the specificity of *E.coli* RF–mRNA crosslink formation (McCaughan *et al*., 1998). In a recent review (Poole and Tate, 2000), it was mentioned that a crosslink was identified in the structural domain D of RF2, near to, or within, the Ser-Pro-Phe motif.

eRF1s display low, if any, sequence similarity with prokaryotic RF1 and RF2 (Frolova *et al*., 1994). The domain organization of human eRF1 established on the basis of its crystal structure (Song *et al*., 2000) and from biochemical studies (Frolova *et al*., 2000) supports the 'tRNA analog' concept (Moffat and Tate, 1994). It has been suggested that the N-terminal (N) domain mimics the anticodon arm, the middle (M) domain is equivalent to the amino acid acceptor arm and the C-terminal (C) domain is responsible for interaction with the class-2 RF, eRF3 (Ebihara and Nakamura, 1999; Merkulova *et al*., 1999). Deletion of the C domain has no influence on *in vitro* eRF1 activity, and thus the active 'core' is composed of N and M domains (Frolova *et al*., 2000). For the *Saccharomyces cerevisiae* eRF1, mutation of certain amino acid residues of the N domain affected stop codon discrimination (Bertram *et al*., 2000). In some ciliate species, a variant nuclear genetic code is used, affecting the meaning of stop codons. For example, in hypotrich *Euplotes*, UAA and UAG are used as stop codons, whereas

UGA codes for Cys. The fact that, in an *in vitro* release assay (performed with rabbit ribosomes), *Euplotes aediculatus* eRF1 responded to the UAA and UAG stop codons (but not to UGA) demonstrates that eRF1 itself bears stop codon recognition properties (Kervestin *et al*., 2001). Sequence alignment of eRF1s and the search for conserved residues within the N domain, which could vary following the reassignment of stop codons in ciliate eRF1, led to several hypotheses on eRF1 stop codon recognition (Inagaki and Doolittle, 2001; Lehman, 2001; Liang *et al*., 2001; Lozupone *et al*., 2001; Muramatsu *et al*., 2001; Inagaki *et al*., 2002). *In vitro* site-directed mutagenesis studies showed that the left part of the NIKS motif (positions 61 and 62) is important for the conservation of RF activity, whereas its right part (positions 63 and 64) and Arg residues in positions 65 and 68 are involved in ribosome binding (Frolova *et al*., 2002). The omnipotent decoding potential of the eRF1s of variant-code organisms was shown recently to be modulated by the TASNIKS sequence (Ito *et al*., 2002). All the above data focused on the N domain as containing the stop codons recognition site, but they failed to demonstrate that this domain directly contacts the stop codons.

We applied (Chavatte *et al*., 2001) to eukaryotes (rabbit ribosome, human eRF1) the same photocrosslinking strategy as previously used in the study of *E.coli* translation termination (Poole and Tate, 2000). The 42mer mRNA analogs used contain a GAC codon corresponding to $tRNA^{Asp}$, followed by either s^4UGA or the control sense s^4UCA triplet. We demonstrated that, in non-phased ribosomes, both s^4UGA and s^4UCA mRNA analogs yielded very similar crosslinking patterns with rRNA and ribosomal proteins (rPs). In contrast, in phased ribosomes, they yielded different crosslinking patterns on the addition of eRF1. The formation of an eRF1–mRNA crosslink was detected only with s^4UGA. It occurs with both full-length eRF1 and a truncated form lacking the C domain and requires the presence of $tRNA^{Asp}$ (Chavatte *et al*., 2001). Using perfluoroaryl-azido derivatized heptaribonucleotides containing a UCC codon for Phe followed by either a stop UAA or sense CAA codon, Bulygin *et al*. (2002) also observed that the formation of an eRF1–mini-mRNA crosslink on the irradiation of a mixture of 80S ribosome, mRNA analog, eRF1 and $tRNA^{Phe}$ was stop codon dependent.

In the present work, we compared the behavior of mRNA analogs bearing in the appropriate position one of the stop codons s^4UGA, s^4UAA and s^4UAG or a closely related sense codon. The ribosome–mRNA complex was phased in the presence of $tRNA^{Asp}$. To monitor the specificity of this interaction, mRNA constructs were used in which the s^4UGA triplet was 'frameshifted' by one, two or three positions with respect to the Asp codon. The results demonstrate that correctly phased stop codons specifically crosslink with eRF1 within the ribosome. To locate on the eRF1 sequence the oligopeptide(s) that crossreact(s) with stop codons containing s^4U, a procedure was developed that leads to highly purified ^{32}P-labeled eRF1 depleted of mRNA. Specific cleavage of the polypeptide chain of wild-type ^{32}P-labeled eRF1, as well as eRF1 mutants, followed by analysis of the labeled peptides, showed that the Lys-Ser-Arg tripeptide (positions 63–65) in the N domain of human eRF1 is crosslinked to the first position of stop codons.

Results

Specificity of eRF1–mRNA analog crosslink formation

Basically, the *in vitro* system consists of 80S ribosomes, $tRNA^{Asp}$ and mRNA analog. The 42mer to 45mer mRNA analogs are purine-rich to minimize the formation of secondary structure or self-association, which could restrict or prevent their binding to the ribosome and/or their template efficiency. In the middle of their sequence, they all contain (Figure 1A) a GAC codon for Asp, followed, on their 3′ side, either immediately or after a few residues, by a single specifically photoactivatable residue, s^4U. The behavior of the ribosome programmed with a 5′-end ^{32}P-labeled mRNA analog containing the GACs^4UGA (UGA mRNA) sequence is represented in Figure 2, which shows the patterns of crosslinks obtained in the absence of $tRNA^{Asp}$ and eRF1 (non-phased ribosomes), in the presence of $tRNA^{Asp}$ (phased ribosomes) and in the presence of $tRNA^{Asp}$ and eRF1. The addition of $tRNA^{Asp}$ to the non-phased ribosomes increases the overall yield of crosslink formation (i.e. the fraction of added mRNA involved in crosslinks) from 5 to 50%, and this is mainly due to the enhancement of rRNA–mRNA crosslinks (apparent mass >100 kDa) and a 19 kDa rP–mRNA (34 kDa) crosslink (Chavatte *et al*., 2001). The transition from the non-phased to phased ribosome is achieved at 0.5 μM $tRNA^{Asp}$, as no further changes in either yield or pattern of crosslink occur at higher $tRNA^{Asp}$ concentrations (data not shown). The addition of eRF1 to the phased ribosomes (Figure 2, lanes 3 and 4) results in significant quenching of all crosslinks (final yield close to 6%), with the exception of the 68–70 kDa one (lanes 3 and 4). The corresponding bands are weak (lane 1) or close to background (lane 2) in the absence of eRF1, but they are strongly stimulated in its presence (lanes 3 and 4). It has been unambiguously shown that this enhancement is due to the formation of the eRF1–mRNA crosslink (Chavatte *et al*., 2001). This finding strongly suggests that, on binding to the correctly programmed ribosomes, eRF1 is in contact with the first position of the stop codon (s^4U), while preventing the s^4U residue from crosslinking with neighboring rRNA and rP. Moreover, the final patterns are identical whether the eRF1 concentration is 2 or 6 μM (compare lanes 3 and 4).

To examine whether other stop codons are able to crosslink with eRF1 on phased ribosomes, 42mer mRNA analogs that contained the s^4UAA or s^4UAG codon in place of s^4UGA (UAA and UAG mRNA analogs) were synthesized. As a control in these experiments, a set of sense codons related to the stop codons (UGG, UCA and UAC mRNA analogs) were used. As the pattern of crosslink with the rPs is sensitive to the ribosome preparation (Chavatte *et al*., 2001), the UGA mRNA analog was always tested in parallel as an internal reference. With the phased ribosomes, all these mRNA analogs yielded the same pattern of crosslinks as for the UGA mRNA (Figure 3A, lane 1). With 6 μM eRF1, the resulting patterns can be subdivided into three types: (i) when any of the stop codons is located at the A site,

A

UGA : 5'-GGGAGAAAAAAGAAAGAAGACs^4**UGA**AAAGAAAAAAAAGAAAAA-3'
UAG : 5'-GGGAGAAAAAAGAAAGAAGACs^4**UAG**AAAGAAAAAAAAGAAAAA-3'
UAA : 5'-GGGAGAAAAAAGAAAGAAGACs^4**UAA**AAAGAAAAAAAAGAAAAA-3'
UCA : 5'-GGGAGAAAAAAGAAAGAAGACs^4**UCA**AAAGAAAAAAAAGAAAAA-3'
UGG : 5'-GGGAGAAAAAAGAAAGAAGACs^4**UGG**AAAGAAAAAAAAGAAAAA-3'
UAC : 5'-GGGAGAAAAAAGAAAGAAGACs^4**UAC**AAAGAAAAAAAAGAAAAA-3'
UGA+1 : 5'-GGGAGAAAAAAGAAAGAAGACGs^4**UGA**AAAGAAAAAAAAGAAAAA-3'
UGA+2 : 5'-GGGAGAAAAAAGAAAGAAGACGGs^4**UGA**AAAGAAAAAAAAGAAAAA-3'
UGA+3 : 5'-GGGAGAAAAAAGAAAGAAGACGGGs^4**UGA**AAAGAAAAAAAAGAAAAA-3'

B

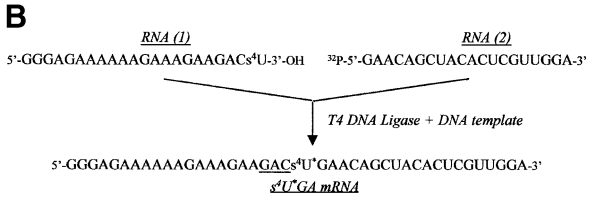

Fig. 1. mRNA containing s^{4}U. (**A**) mRNAs obtained by *in vitro* transcription in the presence of s^{4}UTP (instead of UTP). All 42mer mRNAs contain a GAC codon (underlined) followed by a stop or sense codon (bold). As they differ only by the nature of the latter codon, they were named accordingly. In UGA+1, UGA+2 and UGA+3, the triplet was 'frameshifted' relative to the GAC codon by the insertion of one, two or three Gs, respectively. All these mRNAs were used after 5′-end ^{32}P-labeling. (**B**) Scheme showing the synthesis of the internally labeled s^{4}U*GA mRNA analog. This 42mer mRNA was assembled from two fragments: RNA(1), obtained by *in vitro* transcription; and RNA(2), synthesized chemically. Ligation was performed in the presence of complementary DNA template and T4 DNA ligase.

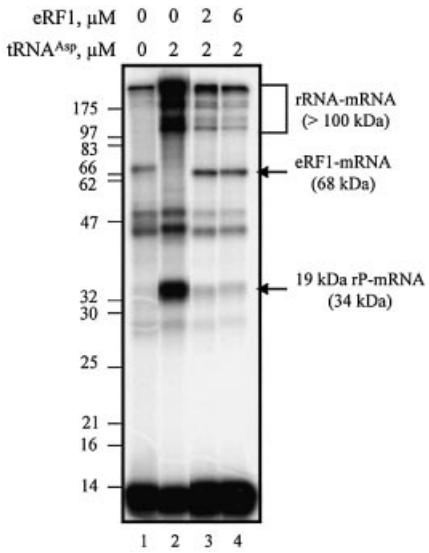

Fig. 2. Dependence of crosslink formation on s^{4}UGA programmed ribosomes as a function of eRF1 concentration. Autoradiograph of the crosslink pattern obtained after irradiation of 0.1 μM 5′-end ^{32}P-labeled s^{4}UGA mRNA analog with 0.2 μM reassociated ribosomes and with or without 2 μM tRNA^{Asp} and variable amounts of eRF1. The irradiated mixtures were analyzed by 10% SDS–PAGE. Lanes 1 and 2 are typical of non-phased and phased ribosome–mRNA complexes. Lanes 3 and 4 show the behavior of the phased ribosomes on the addition of different amounts of eRF1. Molecular mass markers are indicated (in kDa).

the eRF1–mRNA crosslinks are formed (Figure 3A, lanes 2–4), though with different efficiencies (Figure 3B), and the 19 kDa rP–mRNA or rRNA–mRNA crosslinks are severely quenched; (ii) when the s^{4}UCA and s^{4}UAC sense codons are located at the A site, no eRF1–mRNA crosslinks (the 68–70 kDa band corresponds closely to the background values observed in the absence of eRF1) are detected, and the formation of the rRNA–mRNA and 19 kDa rP–mRNA crosslinks is partly quenched; and (iii) the sense s^{4}UGG triplet allows eRF1–mRNA crosslink formation (Figure 3A and B), but quenching of rRNA–mRNA and 19 kDa rP–mRNA crosslinks is less efficient than with stop codons.

To probe more deeply the specificity of eRF1–mRNA crosslink formation, we examined the behavior of a set of mRNA analogs derived from the 42mer UGA mRNA by the insertion of one, two or three G residues between the GAC and the s^{4}UGA triplets, yielding 43mer UGA+1, 44mer UGA+2 and 45mer UGA+3 mRNA analogs, respectively (Figure 1A). In the non-phased ribosomes, all these mRNA analogs yield patterns of crosslinks very similar to those obtained with the UGA mRNA analog, taking into account the respective masses of the mRNAs (data not shown). Incubation with tRNA^{Asp} to phase the ribosomes increases the overall yield of crosslinks in every case (data not shown). It should place the Gs^{4}UG triplet (UGA+1 mRNA), the GGs^{4}U triplet (UGA+2 mRNA) and GGG triplet (UGA+3 mRNA analogs) within the ribosomal A site. Interestingly, the yields of crosslinks with rRNA and 29 and 32 kDa rPs remain unchanged (Figure 4, bands a–c). On the other hand, the formation of the crosslink with the 19 kDa rP (Figure 4, band d) is observed with UGA and UGA+1 mRNA, whereas the crosslink with the 13 kDa rP (Figure 4, band e) is observed almost exclusively with the UGA+1, UGA+2 and UGA+3 mRNA analogs. These data provide strong additional evidence for phasing of the mRNA analogs onto the ribosome on the addition of tRNA^{Asp}. The addition of eRF1 to the phased ribosomes (Figure 4, right) markedly decreases the overall crosslinking yield only with the UGA mRNA analog (Figure 4, compare lanes 1 and 5) and much less with any mRNAs analogs containing G insertions. None of the 'frameshifted' mRNAs allow the formation of the eRF1–mRNA crosslink (Figure 4, lanes 6–8).

Labeling of the crosslink on eRF1

The strategy used to map the site of attachment of the mRNA on eRF1 relies on the determination of the size of the ^{32}P-labeled fragments of eRF1 obtained after specific cleavage of the polypeptide chain. This approach is reliable only if performed on a highly purified form of the stop codon–eRF1 crosslink. As the yield of this crosslink is low (close to 1% of added mRNA), it is likely to be contaminated with rP–mRNA and rRNA–mRNA crosslinked products (Figure 3A). To improve resolution and decrease the background level, we developed a procedure that allows further analysis of the ^{32}P-labeled peptides derived from the eRF1–mRNA crosslink. For this purpose, an internally ^{32}P-labeled 42mer s^{4}U*GA mRNA was constructed, because the s^{4}UGA codon was the most efficient in yielding the desired crosslink (Figure 3B). This mRNA analog was assembled by the ligation of the two oligoribonucleotides RNA(1) and RNA(2) in the presence of DNA ligase and a complementary DNA strand, as described previously (Yu, 1999). To improve correct

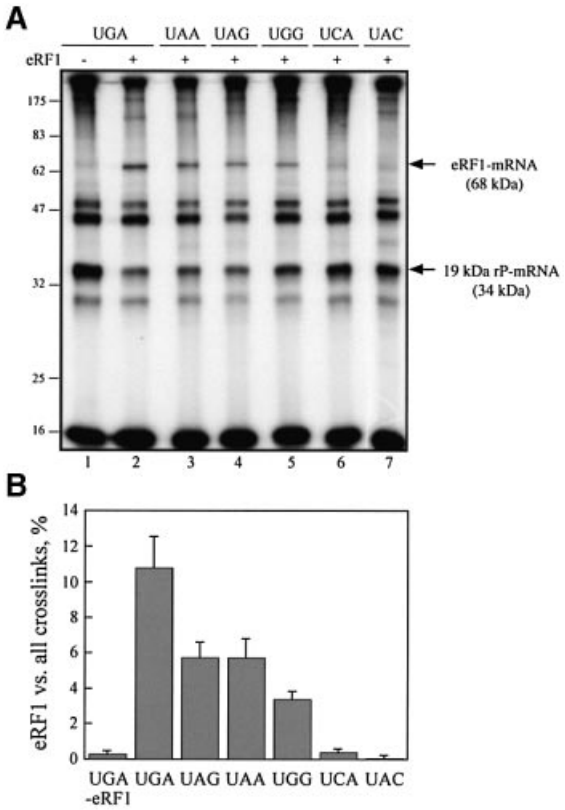

Fig. 3. Codon dependence of eRF1–mRNA and 19 kDa rP–mRNA crosslink formation. (**A**) Autoradiograph of the crosslink patterns obtained with stop or sense codons containing 0.1 μM 42mer mRNA analogs in the presence of 0.2 μM reassociated ribosome, 6 μM eRF1 and 2 μM $tRNA^{Asp}$ (lanes 2–7). For comparison, a control without eRF1 is shown (lane 1). Molecular mass markers are indicated (in kDa) on the left. eRF1–mRNA and 19 kDa rP–mRNA crosslinks are indicated by arrows. (**B**) Codon-dependent formation of the eRF1–mRNA crosslink. The percentage of this crosslink over all of the crosslinks within the same lane was determined by quantification of the data in (A).

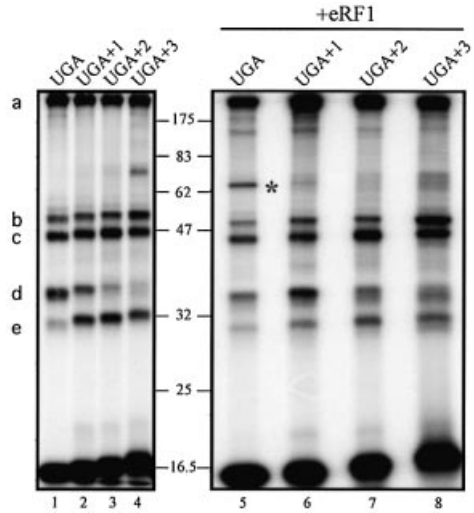

Fig. 4. Crosslink patterns obtained with 'frameshifted' mRNA analogs. 5′-end ^{32}P-labeled frameshifted mRNA (0.1 μM) (Figure 1A) was mixed with 0.2 μM ribosomes and 2 μM $tRNA^{Asp}$ in the absence or presence of 6 μM eRF1. s^4UGA mRNA (lanes 1 and 5) was used as a control. Molecular mass markers are indicated (in kDa). The nature of the crosslinks is indicated on the left: (a) >100 kDa rRNA–mRNA, (b) 32 kDa rP–mRNA, (c) 29 kDa rP–mRNA, (d) 19 kDa rP–mRNA and (e) 13 kDa rP–mRNA; the eRF1–mRNA crosslink is marked by an asterisk.

hybridization, the RNA(1) sequence was identical to the corresponding 5′ part of the parent s^4UGA mRNA analog, whereas the RNA(2) sequence was enriched in pyrimidine residues as compared with the 3′ part of the parent analog (Figure 1B). Prior to ligation, RNA(2) was ^{32}P-labeled at its 5′ end. Thus, after ligation, the label was introduced 3′ of the s^4U probe. Digestion with micrococcal nuclease of the crosslinked complexes obtained with this mRNA analog is expected to remove all mRNA and rRNA–mRNA contaminants while leaving a ^{32}P-labeled residue attached to the crosslinks formed with proteins.

As ligated s^4UGA mRNA differs from the UGA mRNA analog in the 3′ part of its sequence and in the position of the label (Figure 1), its behavior was first examined under previously defined conditions (Figure 2). After irradiation of the s^4U*GA ribosome–mRNA–$tRNA^{Asp}$ ternary complex in the presence of eRF1, one aliquot was treated as usual and the other was digested with micrococcal nuclease prior to SDS–PAGE analysis. The data obtained in a typical experiment are shown in Figure 5. First, they show that the internally labeled mRNA behaves exactly as its 5′ end-labeled analog (compare lane 1 in Figure 5 with lanes 3 and 4 in Figure 2). Secondly, they demonstrate that the nuclease treatment greatly improves the separation of ^{32}P-labeled proteins on the gel. In particular, the 68 kDa band previously shown to correspond either to an rP–mRNA crosslink (in the absence of eRF1) or to, essentially, an eRF1–mRNA crosslink (when eRF1 was added) is now resolved after nuclease treatment into 52 and 55 kDa bands (Figure 5, lane 2). To unambiguously identify the eRF1 band, we took advantage of the presence of a His-tag fused to the N-terminus of eRF1. An aliquot of phased ribosomes containing eRF1 was loaded onto an Ni-NTA column after irradiation and nuclease treatment. The fraction eluted in the presence of 150 mM imidazole was then concentrated and analyzed on the gel (Figure 5, lane 3), demonstrating that the 55 kDa band corresponds to ^{32}P-labeled eRF1 (eRF1p*). Thus, under the conditions used, ligated s^4U*GA mRNA digestion is complete and the procedure makes it possible to isolate purified eRF1p*.

Mapping of the crosslink on the eRF1 protein

To map the crosslink, eRF1p* was either purified by the Ni-NTA column, or the band corresponding to eRF1 (Figure 5, lane 2) was cut from a dried gel. None of these preparations revealed significant contamination by rPp* crosslinks, as shown for the sample purified by the Ni-NTA column (Figure 5, lane 3). Treatment of eRF1p* with CNBr, which cleaves the polypeptides after Met residues (nine sites available in wild-type human eRF1), and subsequent analysis by SDS–PAGE (Figure 6A, lane 1) revealed two major labeled polypeptides of 15.5 and 17.5 kDa (apparent masses) in a 2:1 ratio. From the positions of Met residues along the eRF1 sequence (Figure 6B), it can be inferred that the 15.5 kDa polypeptide is the 52–195 fragment, whereas the 17.5 kDa polypeptide corresponds to the 35–195 fragment. This interpretation was verified as follows. (i) eRF1p* was

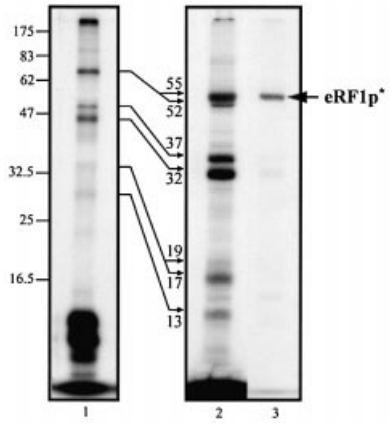

Fig. 5. Crosslink patterns obtained with internally labeled s^4U*GA mRNA analog and phased ribosomes in the presence of eRF1: lane 1, without nuclease treatment; lane 2, after micrococcal digestion of tRNAs. Reaction conditions: 0.1 μM mRNA, 0.2 μM ribosome and, where indicated, 2 μM $tRNA^{Asp}$ and 6 μM eRF1. Autoradiogram after 12.5% SDS–PAGE. To localize the His_6-tagged eRF1p* product (arrow), an aliquot of the mixture obtained after irradiation of the complete mixture was nuclease treated and passed through an Ni-NTA column. The fraction eluted with 150 mM imidazole was analyzed in parallel (lane 3). Molecular masses of the rPp* and eRF1p* obtained after nuclease digestion are indicated (in kDa) close to the thin arrows.

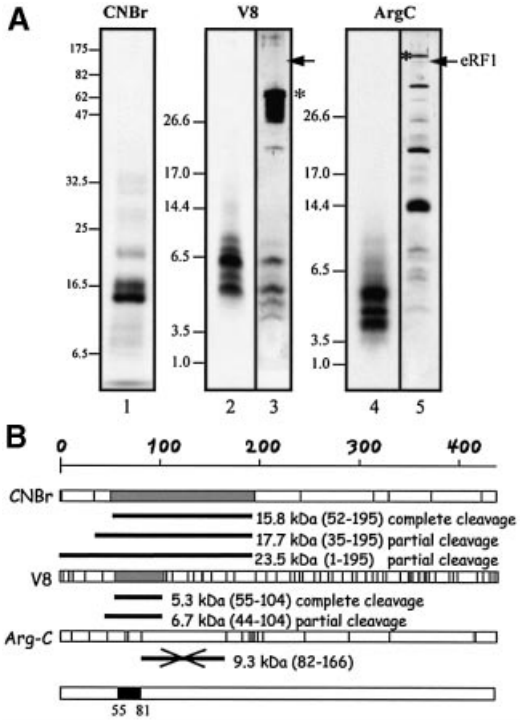

Fig. 6. Mapping the crosslinking site on wild-type eRF1. (**A**) Determination of the size of the ^{32}P-labeled eRF1p* fragments after specific treatments. In lanes 1, 2 and 4, eRF1p* was treated by CNBr (Met↓X), protease V8 (Glu↓X and Asp↓X) and protease Arg-C (Arg↓X), respectively. Samples were analyzed by either 12.5% Tris–glycine (lane 1) or 16.5 % Tris–tricine (lanes 2–5) SDS–PAGE. Digestion of 15 μg of eRF1 with either V8 (lane 3) or Arg-C (lane 5) proteases followed by visualization by silver staining. Asterisks indicate the positions of V8 and Arg-C on the gel. Arrows indicate the position of full-length eRF1. (**B**) Schematic representation of the sites of cleavage of full-length human eRF1by CNBr or V8 and Arg-C proteases; sites are represented as vertical bars. The size of ^{32}P-labeled peptides in agreement with the data of (A) are shown in gray (fragments resulting from complete cleavage) or as black bars (incomplete cleavage) for CNBr and V8. The data obtained with Arg-C show that the 9.3 kDa peptide, positions 82–166 (crossed black bar), is not labeled. Compilation of the data is shown as a black box (positions 55–81 of human eRF1).

subjected to limited CNBr cleavage, leaving intact up to 70% of the initial protein. The polypeptides containing the His-tag were selected using an Ni-NTA column and analyzed by SDS–PAGE; the shortest labeled fragment migrated as an ~25 kDa band, corresponding to the N-terminal fragment up to position 195 (theoretical mass ~24 kDa). (ii) Treatment of free eRF1 by CNBr generated the expected peptides (80% yield) plus fragments resulting from incomplete cleavage, as shown by mass spectrometry and gel analysis followed by silver staining (data not shown).

Proteolytic fragmentation of eRF1p* was also performed with either endoproteinase V8, which cuts after Glu and Asp residues (64 sites available in human eRF1), or Arg-C, which cuts after Arg residues (18 sites available) (Figure 6B). Digestion of free unlabeled eRF1 was examined in parallel. SDS–PAGE analysis showed that protease V8 efficiently cuts free eRF1 (Figure 6A, lane 3), which is no more detectable on the gel, and yielded 6.7–5.3 kDa fragments. Mass spectra confirmed their presence, together with a number of smaller fragments (data not shown). In the eRF1p* V8 digest, both 6.7 and 5.3 kDa fragments plus other minor fragments were strongly labeled (Figure 6A, lane 2), suggesting that the label was attached between positions 56 and 104 (Figure 6B). Arg-C digestion of eRF1p* yielded mainly 4, 4.5 and 5.5 kDa polypeptides, excluding the possibility that the label is attached between positions 82 and 166, which would have generated a polypeptide of 9.3 kDa and longer fragments. Taken together, the data imply that the site of crosslinking maps between positions 55 and 81 in the N domain of eRF1 (Figure 6B).

To refine the position of the crosslink, a strategy based on the CNBr treatment of eRF1 mutants bearing substitution of a single amino acid for Met in the region of interest (positions 55–81) was used. Cleavage on the N-terminal side of the labeled crosslink will generate a large labeled fragment (13–15 kDa), whereas cleavage on its C-terminal side will yield fast-migrating labeled peptides (1–2.5 kDa). Mutations (S60M, V66M and G73M) were performed in non-conserved positions of eRF1. All the corresponding mutant proteins retain full crosslinking ability but variable RF activity (Table I). CNBr cleavage yields a large labeled fragment (~15 kDa) with S60M, whereas it generates fast-migrating polypeptides with V66M and G73M (Figure 7A), showing that the crosslink maps between positions 61 and 66.

For further refinement of the crosslink positions, I62M, K63M and S64M eRF1 mutants were constructed, some of which are affected in either their RF activity or crosslinking ability (Table I). I62M is significantly impaired in its RF activity but crosslinks well. On CNBr treatment, it generates two large labeled polypeptides (Figure 7). The smaller 15.5 kDa fragment migrates faster than the 52–195 fragment obtained with wild-type eRF1 and thus corresponds to a 63–195 labeled polypeptide. It should be noticed that the cleavage efficiency at position 62 is reduced ~2-fold. K63M crosslinks poorly and, on CNBr cleavage, yields a pattern identical to the one obtained

Table I. Percentage crosslinking yields (obtained with internally labeled s^4U*GA mRNA analog) and RF activity of Met mutants relative to wild-type eRF1

	Wild type	S60M	I62M	K63M	S64M	V66M	G73M
Crosslink	100	97	95	43	85	98	80
RF activity with UAA	100	100	7	61	100	52	nd
RF activity with UAG	100	100	5	67	100	30	nd
RF activity with UGA	100	100	28	66	100	39	nd

Values are the averages of at least three independent experiments and are given with ±10% (crosslinks) and ±11% (RF activity) precision.
nd, not determined.

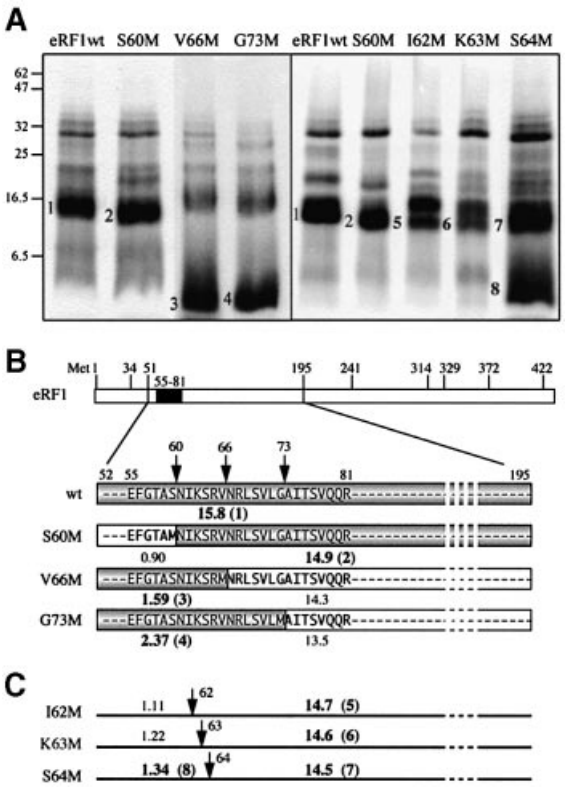

Fig. 7. Mapping of the crosslink with mutant eRF1s. (**A**) Patterns of CNBr induced cleavage fragments obtained with S60M, V66M and G73M (left) and S60M, I62M, K63M and S64M (right). Numbers 1–4 and 5–8 refer to fragments shown in (B) and (C), respectively. Samples were analyzed by 12.5% Tris–glycine SDS–PAGE, and wild-type eRF1p* was used as a control. (**B**) Expected size of ^{32}P-labeled fragments (shown in gray) for S60M, V66M and G73M, indicating that the crosslink maps in the NIKS region. (**C**) Size of fragments expected from CNBr induced cleavage of the 52–195 polypeptide on the substitution of S60, I62, K63 or S64 by a Met residue.

with I62M. On the other hand, S64M generates a fast-migrating labeled peptide with a reduced yield (compare its behavior with that of V66M or G73M). Further analysis of the data above (see Discussion) narrowed the site of crosslink to the KSR peptide (positions 63–65 of human eRF1).

Discussion

Phasing of mRNA onto ribosomes

Basically, our assay includes factor-free rabbit ribosomes and a 42mer to 45mer mRNA analog containing a single photoactivatable s^4U residue but is devoid of an energy source. A 2-fold molar excess of ribosomes over mRNA was used in order to select ribosomes prone to efficient mRNA binding. The characteristic change of the patterns of crosslinks observed on the addition of $tRNA^{Asp}$ to 42mer ribosome–mRNA mixtures (Figure 2) is due to mRNA phasing onto the ribosome. It is well established that, in the presence of its cognate codon, a tRNA exhibits a much higher affinity for the ribosomal P site than for the A or E sites (Graifer *et al*., 1992 and references therein). Therefore, in the phased state of the ribosome–mRNA–$tRNA^{Asp}$ complex, $tRNA^{Asp}$ and its GAC codon are located in the P site, automatically placing the s^4UNN codon of 42mer mRNAs in the A site. This is in agreement with our finding that all 42mer mRNAs yield the same crosslinking patterns both qualitatively and quantitatively (data not shown). 'Frameshifted' s^4UGA mRNAs (Figure 1A) provide additional evidence for correct phasing of the mRNA on the ribosome. Indeed, the left part of Figure 4 shows that the s^4U residue crossreacts with the 19 kDa rP, yielding the 34 kDa crosslink, only when located immediately 3′ to the mRNA decoding site or 3′-shifted by one residue (UGA mRNA and UGA+1 mRNA, Figure 1A). Conversely, it crossreacts with the 13 kDa rP, yielding the 28 kDa crosslink, when it is 3′-shifted by one, two or three residues (UGA+1, UGA+2 and UGA+3 mRNA analogs, respectively).

eRF1 binding to programmed ribosomal A site and eRF1–mRNA crosslink formation

The addition of eRF1 to s^4UGA stop codon programmed ribosomes triggers quenching of all previously observed crosslinks (Figure 3A, lanes 2–4) and the formation of a new 68 kDa band previously identified as an eRF1–mRNA crosslink (Chavatte *et al*., 2001). Obviously, the quenching effect reflects the occupancy of the A site by eRF1, and this is particularly clear for the 34 kDa crosslink (Figure 2). When induced by the addition of 5 μM eRF1, this quenching effect appears to depend solely on the nature of the triplet present in the A site. It is weak but significant (~30%) for the sense codons s^4UCA, s^4UAC (Figure 3) or Gs^4UG (Figure 4), higher (~50%) for s^4UGG and reaches ~70% for the stop codons (Figure 3, lanes 2–4). As shown in Figure 2 (lanes 3 and 4) for UGA mRNA, a 2 μM concentration of eRF1 is sufficient to trigger maximum quenching. These data indicate that stop codons promote strong eRF1 binding to the ribosomal A site as compared with sense codons, whereas the near-cognate s^4UGG triplet adopts an intermediate behavior (a detailed analysis of eRF1 binding isotherms will be published elsewhere). All three stop codons and the near-cognate s^4UGG triplet allow the formation of the eRF1–mRNA crosslink,

whereas only background values are detected with the s^4UCA and s^4UAC codons. The observation that sense codons (except UGG) are unable to promote the formation of the 68 kDa crosslink is confirmed by the data obtained with 'frameshifted' mRNAs (Figure 4). It can thus be concluded that the s^4U-purine-purine triplet programmed A site allows both efficient binding of eRF1 to this site and the formation of the eRF1–mRNA crosslink. Conversion of a single purine residue into pyrimidine markedly decreases the affinity of eRF1 for the A site and prevents the formation of this crosslink. Under *in vitro* conditions, the RF activity of eRF1 was shown to be promoted by stop codons but not by UGG or other sense codons (Frolova *et al*., 1994). In this context, the ability of the s^4UGG triplet to induce an eRF1–mRNA crosslink possibly reflects the lack of sensitivity of the activity assay. Remarkably, UGG stands out as a hot-spot in RF2-dependent termination of protein synthesis in a prokaryotic system (Freistroffer *et al*., 2000), and our data suggest it should behave similarly in the corresponding eRF1-dependent eukaryotic system. In any case, the highly stringent conditions required to observe the formation of an eRF1–mRNA crosslink justifies our attempt to map the crosslink on eRF1.

Identification of the eRF1 crosslinked peptide

Mapping was achieved on wild-type eRF1 in two steps. First, eRF1p* (eRF1 ^{32}P-labeled at the site of the crosslink) was freed from contaminating labeled rPs by SDS–PAGE (Figure 5), or His_6-tagged eRF1p* was directly purified from the irradiated incubation mixture (after nuclease digestion) by affinity chromatography (Figure 5, lane 3). In the second step, purified eRF1p* was specifically cleaved and the size of the resulting fragments was determined (Figure 6A). Taken together, the data show that the crosslink is attached to a fragment that encompasses positions 55–81 (Figure 6B) of eRF1. To narrow the positioning of the crosslink in this region of eRF1, a set of eRF1 mutants was prepared, where a preselected amino acid residue between positions 60 and 73 was substituted for Met. We took advantage of the fact that, on CNBr treatment, the large 52–195 fragment will be asymmetrically cut (Figure 7), thus generating small (0.9–2.4 kDa) and large (⩾13.5 kDa) fragments. If the fast-migrating fragment is labeled, then the crosslink is attached on the N-terminal side of the new cleavage site. S60M, V66M and G73M behave similarly to wild-type eRF1 with respect to their crosslinking ability (Table I). CNBr treatment leads to efficient cleavage at the introduced Met residue (Figure 7A), generating either a large (~15 kDa, band 2 for S60M) fragment or fast-migrating peptides (bands 3 and 4 for V66M and G73M, respectively). These data unambiguously map the crosslink in the highly conserved NIKSR pentapeptide (positions 61–65 of human eRF1). Residue V66 can be excluded from this target site, as the formation of a crosslink involving M66 of V66M would impede CNBr induced cleavage at this position, which is not observed (Figure 7A).

We further attempted to refine the mapping using I62M, K63M and S64M. Their RF activities can be anticipated from earlier data (Frolova *et al*., 2002) and show no apparent correlation with their crosslinking abilities (Table I). After CNBr treatment, I62M and K63M generate very similar patterns (Figure 7), indicating that cleavage occurs at the inserted Met, yielding 14.7 kDa (band 5, I62M) and 14.6 kDa (band 6, K63M) labeled fragments. On the other hand, S64M yields a large 14.5 kDa fragment (band 7) and a fast-migrating one (band 8). These data should be interpreted with caution, as the cleavage yields at inserted Met residues are 2-fold lower than observed with either wild-type eRF1 or S60M and V66M (Figure 7A), which could be due to partial oxidation of the introduced Met by a short-lived O_2 singlet ($^1O_2$) generated during the irradiation step by the closely positioned s^4U residue (reviewed in Favre, 1990). Cleavage might also be prevented if the considered Met is involved in the crosslink. Taking the above considerations into account, it can be concluded that I62 does not crossreact with s^4U, as no fast-migrating peptide could be detected with K63M (Figure 7A). On the other hand, a labeled fragment of 14.5 kDa is observed with S64M, which suggests that some ^{32}P label may be attached to R65. Taken together, these data restrict the site of crosslink to the KSR tripeptide (positions 63–65 of human eRF1). K63M protein is the only one exhibiting a markedly decreased crosslinking ability (Table I), suggesting that the anomalous behavior of K63M is due essentially to the low reactivity of M63, which favors s^4U crosslinking with S64 and R65. This strongly points to K63 as the main site of attachment of the s^4U residue in wild-type eRF1.

An excited s^4U residue crossreacts efficiently only if it is able to come into contact (3–4 Å) with reactive acceptor groups with a favorable orientation (Favre, 1990; Favre *et al*., 1998). Thus, the photocrosslinking procedure used does not necessarily detect all residues susceptible to interaction with s^4U. In this context, the low yield of formation of the eRF1–mRNA crosslink (~1% of total mRNA but 6–15% of the crosslinks formed in the presence of eRF1) is most likely to be due to the sequestration of s^4U when bound to eRF1, thus preventing favorable contacts with neighbor groups. This view is supported by the severe quenching of crosslinks observed on the occupancy of the A site by eRF1 (Figures 2 and 3A). Thus, it can be safely concluded that residues of the NIKSR loop, and particularly K63, participate in the recognition of the invariant U of stop codons.

Crosslinking data and hypotheses on eRF1 stop codon recognition

The resemblance between eRF1 and tRNA is based primarily on the functional similarity between both macromolecules. In particular, both occupy the correctly programmed ribosomal A site, recognizing a specific set of codons (stop and sense codons, respectively), and both are known to act at the ribosome peptidyl transferase center to trigger either release of the polypeptide or peptide bond formation. This resemblance is also supported by the similar shapes of eRF1 and tRNA (Figure 8A and B) and of tRNA and the prokaryotic ribosome recycling factor (Selmer *et al*., 1999; Kim *et al*., 2000; Toyoda *et al*., 2000; Fujiwara *et al*., 2001; Yoshida *et al*., 2001). As eRF1 consists of three domains (Song *et al*., 2000), the major problem still remains to assign the N and M domains relative to the anticodon and acceptor arms of the tRNA, as this cannot be determined solely on the basis of X-ray data. Our finding that the first position of stop codons specif-

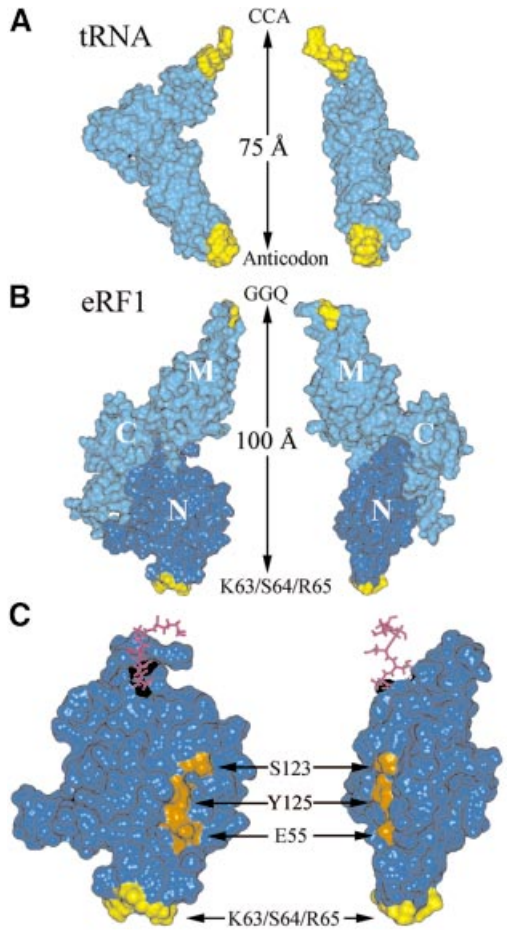

Fig. 8. Comparison of the tRNA (**A**) and eRF1 (**B**) crystallographic structures. The similarity of the structures is shown by a side view (left) and a front view (right). Regions displaying similar roles (anticodon versus KS and CCA versus GGQ) are colored yellow. Molecular structures are shown by their water accessible surfaces, and the N domain is dark blue. (**C**) Enlarged view of the N domain of eRF1 showing the relative positions of the site of crosslink (yellow) and of residues E55, S123 and Y125 (orange), previously proposed to contact the base moiety of the invariant U residue of stop codons (Bertram *et al*., 2000; Muramatsu *et al*., 2001, Inagaki *et al*., 2002). Pink sticks show amino acids connecting the N and M domains.

ically crossreacts with the KSR tripeptide (positions 63–65 of human eRF1; Figure 7) provides the first direct evidence that the N domain does mimic the anticodon arm, as was proposed, but not proven, previously (Bertram *et al*., 2000; Song *et al*., 2000; Ito *et al*., 2002). This tripeptide is located in a short loop surrounded by two helices (α2 and α3), which reinforces the topological similarity with the anticodon loop located at the end of a double helix (Figure 8). Our data also strongly support the assignment of the M domain as equivalent to the acceptor arm of tRNA (Song *et al*., 2000), based on the observation that this domain contains a highly conserved and functionally important GGQ motif, probably involved in triggering peptidyl-tRNA hydrolysis at the peptidyl transferase center of the ribosome (Frolova *et al*., 1999; Seit-Nebi *et al*., 2001).

Several models describing the interaction of stop codons with the N domain of eRF1 have been proposed on the basis of either mutagenesis studies (Bertram *et al*., 2000) or eRF1 sequence alignments (Nakamura *et al*., 2000; Muramatsu *et al*., 2001; Inagaki *et al*., 2002). In the cavity-binding model of Bertram *et al*. (2000), the invariant U in the first position of stop codons is expected to contact Met51 and Ser123, whereas, in the anticodon-mimicry model of Muramatsu *et al*. (2001), it was positioned close to Glu55. Analysis of the primary structure of the eRF1 family, combined with the estimation of the evolutionary rates at amino acid sites, allowed Inagaki *et al*. (2002) to infer that the invariant U might bind to a pocket defined by Glu55, Val71, Tyr125 and Cys127. As shown in Figure 8C, the proposed sites of contact are far removed from the KSR region in the crystallographic structure of eRF1, and thus none of these models appear consistent with our data.

In contrast, our data strongly suggest that K63 and, possibly, neighbor residues of the NIKSR loop are involved in the binding and recognition of the first position of stop codons, and this is consistent with other findings. (i) Amino acid residues of this loop are either strictly conserved, such as I62, or among the slowest evolving residues of eRF1s (Lozupone *et al*., 2001; Inagaki *et al*., 2002). It makes sense that the invariant U of stop codons binds to a relatively well conserved region of eRF1. (ii) N61 and I62 appear to be important for eRF1 release activity, as mutations at these sites impedes it but do not provide critical discrimination among the three stop codons (Frolova *et al*., 2002; Table I). (iii) The decoding capacity of eRF1s can be modulated by the interaction of the TAS (KAT) tripeptides located immediately upstream of the NIKS region (Ito *et al*., 2002). In the crystallographic structure of eRF1, the distance between the NIKS and GGQ motifs is larger than between the corresponding anticodon and CCA region of tRNA (100 versus 75 Å), as shown in Figure 8. This implies a conformational change of eRF1 when bound to a stop codon programmed A site in order to allow the GGQ motif to contact the peptidyl transferase center on the large subunit. The identification of the eRF1 residues contacting the second and third positions of stop codons, which could be readily achieved using a photoactivatable G analog (s^6G) and applying the methodology developed here, is required before this model is fully consistent.

Materials and methods

Synthesis of s^4U modified mRNAs

Oligonucleotides used as mRNAs (and presented in Figure 1A) were synthesized by *in vitro* transcription of synthetic DNA templates (Genset, Paris, France) with T7 RNA polymerase, as described previously (Chavatte *et al*., 2001). The nucleotide triphosphate mixture was composed of ATP, GTP, CTP and s^4UTP (Amersham Pharmacia Biotech). UTP was replaced by s^4UTP, allowing the incorporation of the s^4U probe in the single position available. These mRNAs were 5′ end-labeled with [γ-^{32}P]ATP (ICN) by polynucleotide kinase. They were purified by 15% PAGE, eluted and ethanol precipitated.

The internally labeled s^4U*GA mRNA was assembled by the ligation of the two fragments RNA(1) and RNA(2) following a previously described procedure (Sontheimer, 1994; Yu, 1999). RNA(1) synthesized by *in vitro* transcription (see above) contained a single s^4U residue at its 3′ end. RNA(2) (Eurogentec) was ^{32}P-labeled at its 5′ end with T4 polynucleotide kinase. Both oligonucleotides were hybridized to the same DNA template (Figure 1C), and phosphodiester bond formation was catalyzed by T4 DNA ligase. Thus, 40 pmol of RNA(1), 30 pmol of ^{32}P-labeled RNA(2) and 40 pmol of DNA template were incubated overnight at 37°C in 50 mM Tris–HCl pH 7.6, 10 mM $MgCl_2$, 1 mM ATP,

1 mM DTT and 5% (w/v) polyethylene glycol-8000 (final volume 30 µl), together with 15 U of T4 DNA ligase, allowing the formation of 15–20 pmol of ligated s^4U*GA mRNA. The 42mer mRNA was then purified by 15% PAGE.

Ribosomes and yeast tRNA^{Asp}

Isolation and purification of 80S reticulocyte ribosomes was performed as described previously (Frolova *et al*., 1998). Standard 80S ribosomes washed by 0.5 M KCl ('high salt-washed' ribosomes) were purified by centrifugation through a 20% sucrose cushion and further purified by dissociation into subunits and subsequent reassociation (reassociated ribosomal subunits). Yeast tRNA^{Asp} gene transcript was obtained by *in vitro* transcription (16 h at 37°C) of a linearized plasmid (derived from pUC19) in which the T7 RNA polymerase promoter region was directly connected to the downstream tRNA sequence (Frugier *et al*., 1993).

Cloning and mutagenesis of human eRF1

The full-length cDNA encoding human eRF1 carrying His-tag at the N-terminus was cloned in pQE30 vector (Qiagen), as described previously (Frolova *et al*., 1998, 2000). For site-directed mutagenesis, the full-length cDNA encoding human eRF1 with the C-terminal His-tag was cloned into pET23b(+) vector (Novagen), as described previously (Seit-Nebi *et al*., 2001; Frolova *et al*., 2002). The mutagenesis procedure generating eRF1 mutants was performed according to the PCR-based 'megaprimer' method (Sarkar and Sommmer, 1990), as described previously (Frolova *et al*., 2002). The primers used for the generation of eRF1 mutants are the following: S60M, 5′-ACTGCAATGAACA-TTAAGTCACGA-3′; I62M, 5′-CTCGTGACTTCATGTTAGATGC-3′; K63M, 5′-GTTTACTCGTGACATAATGTTAGATG-3′; S64M, 5′-GG-TTTACTCGCATCTTAATGTTAG-3′; V66M, 5′-TCACGAATGAAC-CGCCTTTCAGTCC-3′; and G73M, 5′-GTCCTGATGGCCATTACAT-CTGTAC-3′.

Expression and purification of human eRF1 and assay for RF activity

Wild-type human eRF1 and its mutants were expressed in *E.coli* strain BL21(DE3), purified using Ni-NTA resin (Superflow, Qiagen), and RF activity was measured as described previously (Frolova *et al*., 1994, 2000).

Crosslinking procedures

The standard *in vitro* system was composed of 0.1 µM ^{32}P-labeled mRNA, 2 µM tRNA^{Asp}, 0.2 µM high-salt-washed or reassociated (when mentioned in figure legends) 80S ribosomes and variable amounts of eRF1 (≤6 µM) in a final volume of 10 µl. The irradiation buffer contained 50 mM Tris–HCl pH 7.4, 100 mM KCl, 10 mM $MgCl_2$ and 1 mM DTT. Each sample was incubated for 1 h at 37°C, placed into a siliconized glass capillary tube and irradiated for 30 min at 4°C. The light source was an HBO 150 W superpressure mercury lamp placed 5 cm from the sample and providing near-ultraviolet light (>320 nm), because shorter wavelengths were removed using an MTO J320A filter. These conditions allowed the completion of the crosslinking reactions. The irradiated sample was diluted in dye buffer and then resolved by 10% SDS–PAGE. The gel was then dried and analyzed on a PhosphorImager (Molecular Dynamics). Pre-stained molecular weight markers were systematically analyzed on a parallel lane of the gel. Crosslinks were counted using Image-Quant software.

eRF1 mapping

Ligated s^4U*GA mRNA was prepared just before the irradiation procedure in order to prevent radiolysis. s^4U*GA (0.1 µM) mRNA was mixed with 0.2 µM ribosomes, 2 µM tRNA^{Asp} and 5 µM eRF1 in a final volume of 50 µl of irradiation buffer. Crosslinking was performed as described above. The irradiated sample was then diluted in nuclease buffer containing 50 mM Tris–HCl pH 8.8 and 10 mM $CaCl_2$. Micrococcal nuclease (1 U, MBI Fermentas) was added, allowing complete RNA digestion after 2 h at 37°C. Two procedures were used to separate eRF1 from other labeled proteins (and RNA fragments). (i) The nuclease activity was stopped by the addition of dye buffer containing EDTA, and the mixture was subjected to 12.5% SDS–PAGE. The gel was dried and analyzed by autoradiography, and the band corresponding to eRF1p* was excised. (ii) The mixture containing His_6-tagged eRF1 was loaded onto an Ni-NTA column (Superflow). The column was first washed with 200 vol. of IMAC 10 (20 mM Tris–HCl pH 8, 0.2 M KCl, 10% glycerol and 10 mM imidazole). His_6-tagged eRF1 was then eluted with IMAC 150 (20 mM Tris–HCl pH 8, 0.2 M KCl, 10% glycerol and 150 mM imidazole). The corresponding fractions were pooled and precipitated with ethanol (final concentration 66% v/v).

The purified eRF1p* was digested directly in the gel slice or in solution by overnight reaction with CNBr (a few crystals) in 100 µl of 70% formic acid at room temperature, with 5 µg of endoproteinase V8 (Roche Biochemicals) in 50 µl of 25 mM sodium phosphate buffer pH 7.8 at 25°C, or with 0.5 µg of endoproteinase Arg-C in 50 µl of incubation mixture (Roche Biochemicals) at 37°C. After the reaction with CNBr, the sample was dried and then diluted in equilibration dye buffer and analyzed by 12.5% Tris–glycine SDS–PAGE in parallel with molecular weight markers ranging from 6.5 to 175 kDa (Figure 6A). The products of enzymatic digestions were diluted in dye buffer and analyzed by 16.5% Tris–tricine SDS–PAGE in parallel with ultra-low-range molecular weight markers ranging from 1.1 to 26.6 kDa (Sigma). The gels were dried and analyzed by autoradiography. As a control of proteolytic activity, 15 µg of eRF1 was digested by either endoproteinase V8 or Arg-C, separated as described above and revealed by Silver Staining Kit Protein (Amersham Pharmacia Biotech).

Acknowledgements

We thank R.Giégé and A.Theolbald-Dietrich for the kind gift of the plasmid used to obtain the yeast tRNA^{Asp} gene transcript, and W.Merrick for the generous gift of rabbit ribosomes. We are grateful to A.Kononenko for his participation in the cloning and purification of mutant eRF1s, and to N.Ivanova and A.Poltaraus for the sequencing of human eRF1 mutant genes. The very kind assistance of A.-L.Haenni in improving the manuscript is acknowledged. The authors are indebted to Professor Lev Kisselev (L.K.) and Dr Luda Frolova (L.F.) for their encouragement throughout this work, which was supported by a 'Chaire Internationale Blaise Pascal' (L.K.), the Human Frontier Science Program (grant R-96-032), INTAS (grant 00-0041), the Russian Foundation for Basic Research (L.K. and L.F.) and the Russian Foundation for Support of Scientific Schools (L.K.). L.C. thanks MENESR and Fondation pour la Recherche Médicale for research fellowships.

References

Bertram,G., Bell,H.A., Ritchie,D.W., Fullerton,G. and Stansfield,I. (2000) Terminating eukaryote translation: domain 1 of release factor eRF1 functions in stop codon recognition. *RNA*, **6**, 1236–1247.

Bertram,G., Innes,S., Minella,O., Richardson,J. and Stansfield,I. (2001) Endless possibilities: translation termination and stop codon recognition. *Microbiology*, **147**, 255–269.

Brown,C.M. and Tate,W.P. (1994) Direct recognition of mRNA stop signals by *Escherichia coli* polypeptide chain release factor two. *J. Biol. Chem.*, **269**, 33164–33170.

Bulygin,K.N., Repkova,M.N., Ven'aminova,A.G., Graifer,D.M., Karpova,G.G., Frolova,L.Yu. and Kisselev,L.L. (2002) Placement of mRNA stop signal towards polypeptide chain release factors and ribosomal proteins in 80S ribosomes. *FEBS Lett.*, **514**, 96–101.

Chavatte,L., Frolova,L., Kisselev,L. and Favre,A. (2001) The polypeptide chain release factor eRF1 specifically contacts the s^4UGA stop codon located in the A site of eukaryotic ribosomes. *Eur. J. Biochem.*, **268**, 2896–2904.

Drugeon,G., Jean-Jean,O., Frolova,L., Le Goff,X., Philippe,M., Kisselev,L. and Haenni,A.L. (1997) Eukaryotic release factor 1 (eRF1) abolishes readthrough and competes with suppressor tRNAs at all three termination codons in messenger RNA. *Nucleic Acids Res.*, **25**, 2254–2258.

Ebihara,K. and Nakamura,Y. (1999) C-terminal interaction of translational release factors eRF1 and eRF3 of fission yeast: G-domain uncoupled binding and the role of conserved amino acids. *RNA*, **5**, 739–750.

Favre,A. (1990) 4-thiouridine as an intrinsic photoaffinity probe of nucleic acid structure and interactions. In Morrison,H. (ed.), *Bioorganic Photochemistry: Photochemistry and the Nucleic Acids*. John Wiley & Sons, New York, NY, pp. 379–425.

Favre,A., Saintome,C., Fourrey,J.L., Clivio,P. and Laugaa,P. (1998) Thionucleobases as intrinsic photoaffinity probes of nucleic acid structure and nucleic acid–protein interactions. *J. Photochem. Photobiol. B*, **42**, 109–124.

Freistroffer,D.V., Kwiatkowski,M., Buckingham,R.H. and Ehrenberg,M. (2000) The accuracy of codon recognition by polypeptide release fctors. *Proc. Natl Acad. Sci. USA*, **97**, 2046–2051.

Frolova,L. *et al.* (1994) A highly conserved eukaryotic protein family possessing properties of polypeptide chain release factor. *Nature*, **372**, 701–703.

Frolova,L.Y., Simonsen,J.L., Merkulova,T.I., Litvinov,D.Y., Martensen,P.M., Rechinsky,V.O., Camonis,J.H., Kisselev,L.L. and Justesen,J. (1998) Functional expression of eukaryotic polypeptide chain release factors 1 and 3 by means of baculovirus/insect cells and complex formation between the factors. *Eur. J. Biochem.*, **256**, 36–44.

Frolova,L.Y., Tsivkovskii,R.Y., Sivolobova,G.F., Oparina,N.Y., Serpinsky,O.I., Blinov,V.M., Tatkov,S.I. and Kisselev,L.L. (1999) Mutations in the highly conserved GGQ motif of class 1 polypeptide release factors abolish ability of human eRF1 to trigger peptidyl-tRNA hydrolysis. *RNA*, **5**, 1014–1020.

Frolova,L.Y., Merkulova,T.I. and Kisselev,L.L. (2000) Translation termination in eukaryotes: polypeptide release factor eRF1 is composed of functionally and structurally distinct domains. *RNA*, **6**, 381–390.

Frolova,L., Seit-Nebi,A. and Kisselev,L. (2002) Highly conserved NIKS tetrapeptide is functionally essential in eukaryotic translation termination factor eRF1. *RNA*, **8**, 129–136.

Frugier,M., Florentz,C., Schimmel,P. and Giege,R. (1993) Triple aminoacylation specificity of a chimerized transfer RNA. *Biochemistry*, **32**, 14053–14061.

Fujiwara,T., Ito,K. and Nakamura,Y. (2001) Functional mapping of ribosome-contact sites in the ribosome recycling factor: a structural view from a tRNA mimic. *RNA*, **7**, 64–70.

Graifer,D.M., Nekhai,S.Yu., Mundus,D.A., Fedorova,O.S. and Karpova,G.G. (1992) Interaction of human and *Escherichia coli* tRNA(Phe) with human 80S ribosomes in the presence of oligo- and polyuridylate templates. *Biochim. Biophys. Acta*, **1171**, 56–64.

Inagaki,Y. and Doolittle,W.F. (2001) Class I release factors in ciliates with variant genetic codes. *Nucleic Acids Res.*, **29**, 921–927.

Inagaki,Y., Blouin,C., Doolittle,W.F. and Roger,A.J. (2002) Convergence and constraint in eukaryotic release factor 1 (eRF1) domain 1: evolution of stop codon specificity. *Nucleic Acids Res.*, **30**, 532–544.

Ito,K., Uno,M. and Nakamura,Y. (2000) A tripeptide 'anticodon' deciphers stop codons in messenger RNA. *Nature*, **403**, 680–684.

Ito,K., Frolova,L., Seit-Nebi,A., Karamyshev,A., Kisselev,L. and Nakamura,Y. (2002) Omnipotent decoding potential resides in eukaryotic translation termination factor eRF1 of variant-code organisms and is modulated by the interactions of amino acid sequences within domain 1. *Proc. Natl Acad. Sci. USA*, **99**, 8494–8499.

Kervestin,S., Frolova,L., Kisselev,L. and Jean-Jean,O. (2001) Stop codon recognition in ciliates: *Euplotes* release factor does not respond to reassigned UGA codon. *EMBO rep.*, **2**, 680–684.

Kim,K.K., Min,K. and Suh,S.W. (2000) Crystal structure of the ribosome recycling factor from *Escherichia coli*. *EMBO J.*, **19**, 2362–2370.

Kisselev,L.L. and Buckingham,R.H. (2000) Translational termination comes of age. *Trends Biochem. Sci.*, **25**, 561–566.

Le Goff,X., Philippe,M. and Jean-Jean,O. (1997) Overexpression of human release factor 1 alone has an antisuppressor effect in human cells. *Mol. Cell. Biol.*, **17**, 3164–3172.

Lehman,N. (2001) Molecular evolution: Please release me, genetic code. *Curr. Biol.*, **11**, R63–R66.

Liang,A., Brunen-Nieweler,C., Muramatsu,T., Kuchino,Y., Beier,H. and Heckmann,K. (2001) The ciliate *Euplotes* octocarinatus expresses two polypeptide release factors of the type eRF1. *Gene*, **262**, 161–168.

Lozupone,C.A., Knight,R.D. and Landweber,L.F. (2001) The molecular basis of nuclear genetic code change in ciliates. *Curr. Biol.*, **11**, 65–74.

McCaughan,K.K., Poole,E.S., Pel,H.J., Mansell,J.B., Mannering,S.A. and Tate,W.P. (1998) Efficient *in vitro* translational termination in *Escherichia coli* is constrained by the orientations of the release factor, stop signal and peptidyl-tRNA within the termination complex. *Biol. Chem.*, **379**, 857–866.

Merkulova,T.I., Frolova,L.Y., Lazar,M., Camonis,J. and Kisselev,L.L. (1999) C-terminal domains of human translation termination factors eRF1 and eRF3 mediate their *in vivo* interaction. *FEBS Lett.*, **443**, 41–47.

Moffat,J.G. and Tate,W.P. (1994) A single proteolytic cleavage in release factor 2 stabilizes ribosome binding and abolishes peptidyl-tRNA hydrolysis activity. *J. Biol. Chem.*, **269**, 18899–18903.

Muramatsu,T., Heckmann,K., Kitanaka,C. and Kuchino,Y. (2001) Molecular mechanism of stop codon recognition by eRF1: a wobble hypothesis for peptide anticodons. *FEBS Lett.*, **488**, 105–109.

Nakamura,Y. and Ito,K. (1998) How protein reads the stop codon and terminates translation. *Genes Cells*, **3**, 265–278.

Nakamura,Y., Ito,K. and Ehrenberg,M. (2000) Mimicry grasps reality in translation termination. *Cell*, **101**, 349–352.

Poole,E. and Tate,W. (2000) Release factors and their role as decoding proteins: specificity and fidelity for termination of protein synthesis. *Biochim. Biophys. Acta*, **1493**, 1–11.

Poole,E.S., Brimacombe,R. and Tate,W.P. (1997) Decoding the translational termination signal: the polypeptide chain release factor in *Escherichia coli* crosslinks to the base following the stop codon. *RNA*, **3**, 974–982.

Sarkar,G. and Sommer,S.S. (1990). The 'megaprimer' method of site-directed mutagenesis. *Biotechniques*, **8**, 404–407.

Seit-Nebi,A., Frolova,L., Justesen,J. and Kisselev,L. (2001) Class-1 translation termination factors: invariant GGQ minidomain is essential for release activity and ribosome binding but not for stop codon recognition. *Nucleic Acids Res.*, **29**, 3982–3987.

Selmer,M., Al-Karadaghi,S., Hirokawa,G., Kaji,A. and Liljas,A. (1999) Crystal structure of *Thermotoga maritima* ribosome recycling factor: a tRNA mimic. *Science*, **286**, 2349–2352.

Song,H., Mugnier,P., Das,A.K., Webb,H.M., Evans,D.R., Tuite,M.F., Hemmings,B.A. and Barford,D. (2000) The crystal structure of human eukaryotic release factor eRF1—mechanism of stop codon recognition and peptidyl-tRNA hydrolysis. *Cell*, **100**, 311–321.

Sontheimer,E.J. (1994) Site-specific RNA crosslinking with 4-thiouridine. *Mol. Biol. Rep.*, **20**, 35–44.

Tate,W., Greuer,B. and Brimacombe,R. (1990) Codon recognition in polypeptide chain termination: site directed crosslinking of termination codon to *Escherichia coli* release factor 2. *Nucleic Acids Res.*, **18**, 6537–6544.

Toyoda,T., Tin,O.F., Ito,K., Fujiwara,T., Kumasaka,T., Yamamoto,M., Garber,M.B. and Nakamura,Y. (2000) Crystal structure combined with genetic analysis of the *Thermus thermophilus* ribosome recycling factor shows that a flexible hinge may act as a functional switch. *RNA*, **6**, 1432–1444.

Vestergaard,B., Van,L.B., Andersen,G.R., Nyborg,J., Buckingham,R.H. and Kjeldgaard,M. (2001) Bacterial polypeptide release factor RF2 is structurally distinct from eukaryotic eRF1. *Mol. Cell*, **8**, 1375–1382.

Weiss,R.B., Murphy,J.P. and Gallant,J.A. (1984) Genetic screen for cloned release factor genes. *J. Bacteriol.*, **158**, 362–364.

Yoshida,T. *et al.* (2001) Solution structure of the ribosome recycling factor from *Aquifex aeolicus*. *Biochemistry*, **40**, 2387–2396.

Yu,YT. (1999) Construction of 4-thiouridine site-specifically substituted RNAs for cross-linking studies. *Methods*, **18**, 13–21.

Received June 5, 2002; revised and accepted July 23, 2002